

q -deformed statistics and the role of a light dark matter fermion in the supernova SN1987A cooling

Atanu Guha,^{1,*} Selvaganapathy. J,^{1,†} and Prasanta Kumar Das^{1,‡}

¹*Department of Physics, Birla Institute of Technology and Science-Pilani,
K. K. Birla Goa campus, NH-17B, Zuarinagar, Goa-403726, India*

(Dated: April 29, 2022)

Abstract

Light dark matter($\simeq 1 - 30$ MeV) particles pair produced in electron-positron annihilation $e^-e^+ \xrightarrow{\gamma} \chi\bar{\chi}$ inside the supernova core can take away the energy released in the supernova SN1987A explosion. Working within the formalism of q -deformed statistics (with the average value of the supernovae core temperature(fluctuating) being $T_{SN} = 30$ MeV) and using the Raffelt's criterion on the emissivity for any new channel $\dot{\epsilon}(e^+e^- \rightarrow \chi\bar{\chi}) \leq 10^{19} \text{ erg g}^{-1}\text{s}^{-1}$, we find that as the deformation parameter q changes from 1.0 (undeformed scenario) to 1.1(deformed scenario), the lower bound on the scale Λ of the dark matter effective theory varies from 3.3×10^6 TeV to 3.2×10^7 TeV for a dark matter fermion of mass $m_\chi = 30$ MeV. Using the optical depth criteria on the free streaming of the dark matter fermion, we find the lower bound on $\Lambda \sim 10^8$ TeV for $m_\chi = 30$ MeV. In a scenerio,where the dark matter fermions are pair produced in the outermost sector of the supernova core (with radius $0.9R_c \leq r \leq R_c$, $R_c(= 10$ km) being the supernova core radius or the radius of proto-neutron star), we find that the bound on Λ ($\sim 3 \times 10^7$ TeV) obtained from SN cooling criteria (Raffelt's criteria) is comparable with the bound obtained from free streaming (optical depth criterion) for light fermion dark matter of mass $m_\chi = 10 - 30$ MeV.

Keywords: Dark matter, Supernova cooling, q -deformed statistics, free-streaming,

*p2014401@goa.bits-pilani.ac.in

†p2012015@goa.bits-pilani.ac.in

‡Author(corresponding):pdas@goa.bits-pilani.ac.in

I. INTRODUCTION

The fact that dark matter plays a very important role in building the universe we live in is gradually gaining ground due to concrete experimental evidence collected over a period of time. In 1933, Fritz Zwicky [1] found that the normal luminous matter is alone not sufficient to explain the velocity dispersion of galaxies in the Coma cluster of galaxies: one requires non-luminous matter, dubbed as dark matter(DM). Current data suggests that DM is five times more than the normal luminous matter in the Universe[2]. Now, the dark matter(DM) does not interact electromagnetically with the normal luminous matter since it(DM) has no electromagnetic charge. Even it does so, it is very weak. So far, scientists have been able to infer the existence of dark matter only through its gravitational effect on normal matter.

But what is dark matter? For a long time it remains a mystery. A wide range of collider and astrophysical study suggests that it is a Weakly Interacting Massive Particle(WIMP) of mass lying in between few MeV to few GeV. Theories suggest that DM candidates are most likely to be found in the beyond the Standard Model(SM) physics, such as supersymmetry and extra dimensions. Direct detection of DM includes its interaction with nucleons in underground detectors, whereas indirect detection through DM annihilation to SM states in the Sun (to neutrinos) has been done. Experiments at the Large Hadron Collider(LHC) and the upcoming electron-positron linear collider(LC) will give more information about the dark matter as the missing energy signature. See [2–4] for a review on dark matter searches.

An enormous amount of gravitational binding energy 10^{53} ergs was released in the supernova SN1987A explosion of which about 99% was carried away by neutrino alone. To understand the supernova energy loss mechanism and its relevance in the beyond standard model physics has been an area of active research for a long time[5]. In 2006, Fayet *et al.*[6] studied the impact of light dark matter on the core collapse supernova cooling and found that the 1 – 30 MeV mass dark matter fermion can explain SN1987A energy loss rate. They also found that if the dark matter particles are of mass $m_\chi \leq 10$ MeV and reproduce the observed dark matter relic density, it would lead to the modification of the supernova cooling dynamics, which is unacceptable. Kadota *et al.*[17] studied the impact of International Linear Collider(ILC) and SN1987A energy loss rate due to the light (MeV) dark matter. They found the SN bound to be more stringent than those obtained from ILC by a factor of $\mathcal{O}(10^5)$ for a DM mass below 100 MeV.

Here we would like to investigate the impact of light dark matter fermions on the energy released in SN1987A explosion. We work in a dark matter model characterized by an effective scale Λ and use the formalism of q -deformed statistics which takes care of the fluctuation of the core temperature of the supernova. While Kadota *et al.*[17] considered the dark matter fermion and SM photon coupling arising from magnetic dipole moment operator, we have generalized our work where a SM photon may couple with dark matter fermion through the magnetic dipole moment operator or electric dipole moment operators or both.

The outline of the work is as follows. We give a brief description of SN1987A cooling problem and a small introduction of q -deformed statistics in section II. In section III, we discuss the dark matter pair production in electron-positron annihilation and find the supernova energy loss rate due to this dark matter fermion pair production. The numerical analysis part is presented in section IV. Using the Raffelt's criterion, we obtain bound on the scale Λ of the effective dark matter theory in deformed($q \neq 1$) and undeformed ($q = 1$) scenarios. Using the optical depth criteria(based on free streaming of dark matter fermions), we obtain constraints on Λ . Finally, we conclude in section V and VI.

II. SUPERNOVA EXPLOSION, ITS COOLING AND q -DEFORMED STATISTICS

A. Supernova cooling, Raffelt's criterion

The supernova SN1987A, a typical example of a core-collapse supernova explosion is the final fate of massive star of mass $M \geq 8 M_{\odot}$. The energy released in SN1987A explosion is enormous: it is the gravitational binding energy E_g of the proto-neutron star (of mass M_{PNS}), given by

$$E_g = \frac{3G_N M_{PNS}^2}{5R_{NS}} \sim 3.0 \times 10^{53} \text{ erg.} \quad (1)$$

Here $M_{PNS} = 1.5M_{\odot}$, $R_{NS} = 10 \text{ Km}$ and G_N is the Newton's gravitational constant. Out of this 99% of the released energy is carried away by neutrinos, while the rest 1% contributes to the kinetic energy of the explosion. To detect this neutrino burst by the earth based detector is of primary astrophysical interest of the core-collapse supernova. About 10^{53} ergs energy was released in the supernova SN1987A explosion in a couple of seconds and two collaborations Kamiokande [7] and IMB[8] first detected this neutrino flux using their earth based detectors. The observed neutrino luminosity in the detector(IMB

or Kamiokande) is $L_\nu \sim 3 \times 10^{53}$ erg s⁻¹ (including 3 generations of neutrinos and anti-neutrinos i.e. ν_e, ν_μ, ν_τ and $\bar{\nu}_e, \bar{\nu}_\mu, \bar{\nu}_\tau$). So $\tilde{L}_\nu = \frac{L_\nu}{6} \sim 3 \times 10^{52}$ erg s⁻¹. The mass of a typical proto-neutron star $M_{PNS} = 1.5M_\odot = 3 \times 10^{33}$ g. So, the average energy loss per unit mass is $\frac{\tilde{L}_\nu}{M_{PNS}} \simeq 1 \times 10^{19}$ erg g⁻¹s⁻¹. Note that this is the energy carried away by each of the above 6 (anti)-neutrino species. Now besides neutrino, if KK graviton, KK radion, axion also take away energy, the energy-loss rate due to these new channels ϵ_{new} should be less than the above average energy loss rate [5] i.e.

$$\epsilon_{new} \leq 10^{19} \text{ erg g}^{-1}\text{s}^{-1} \quad (2)$$

and this follows from the observed neutrino luminosity per species (total 6 neutrino and anti-neutrinos, three type each). So, the upper bound on ϵ_{new} (G. Raffelt's criterion) is a data-driven entity and it does not have an implicit dependence on the fact the ensemble of particles obey the normal Bose-Einstein(BE) statistics or Fermi-Dirac(FD) Statistics characterized by the equilibrium temperature T_{SN} or by Tsallis statistics where the fluctuation around T_{SN} is taken into account. If any energy-loss mechanism has an emissivity greater than 10^{19} erg g⁻¹ s⁻¹, then it will remove sufficient energy from the explosion to invalidate the current understanding of core-collapse supernova.

Using the Raffelt's criteria of the supernova energy loss rate for any new physics channel, we now constrain the scale Λ of the dark matter effective theory. Now since the core temperature of the supernova is fluctuating, we will work here within the formalism of q -deformed statistics[9] where this temperature fluctuation is taken into account.

B. Fluctuating temperature and Tsallis statistics and temperature fluctuation

The temperature (T) fluctuations in the q -deformed statistics [10] takes the χ^2 distribution of the following form

$$f(\beta) = \frac{1}{\Gamma\left(\frac{n}{2}\right)} \left(\frac{n}{2\beta_0}\right)^{n/2} \beta^{\frac{n}{2}-1} \exp\left(-\frac{n\beta}{2\beta_0}\right) \quad (3)$$

where n is the degree of the distribution and $\beta = \frac{1}{kT}$. The average of the fluctuating inverse temperature β can be estimated as

$$\langle\beta\rangle = n\langle X_i^2\rangle = \int_0^\infty \beta f(\beta) d\beta = \beta_0 \quad (4)$$

Taking into account the local temperature fluctuation, integrating over all β , we find the q -generalized relativistic(with particle energy $E = \sqrt{\mathbf{p}^2 c^2 + m^2 c^4}$) Maxwell-Boltzmann distribution

$$\mathcal{P}(E) \sim \frac{E^2}{(1 + b(q-1)E)^{\frac{1}{q-1}}} \quad (5)$$

where $q = 1 + \frac{2}{n+6}$ and $b = \frac{\beta_0}{4-3q}$. It's generalization to Fermi-Dirac and Bose-Einstein distribution is worked out in [11]. The average occupation number of any particle within this q -deformed statistics (Tsallis statistics [9]) formalism, is given by $f_i(\beta, E_i)$ ($i = 1, 2$ corresponds to particles) where

$$f_i(\beta, E_i) = \frac{1}{(1 + (q-1)bE_i)^{\frac{1}{q-1}} \pm 1} \quad (6)$$

where the $-$ sign is for bosons and $+$ sign is for fermions. Note that the effective Boltzmann factor $x_i = (1 + (q-1)bE_i)^{-\frac{1}{q-1}}$ approaches to the ordinary Boltzmann factor $e^{-bE_i} (= e^{-\beta_0 E_i})$ as $q \rightarrow 1$. The q -deformed statistics finds important application in collider physics and astrophysics: Beck *et al.*[12] use the q -deformed statistics in order to explain the measured energy spectrum of primary cosmic rays. With $b^{-1} = kT_0 = 107$ MeV and the deformation parameter $q = 1.215$ and $q = 1.222$, respectively, they were able to explain quite well the flux rate i.e. the upper(upto the knee) portion and the lower (the ankle) portion of the cosmic ray spectrum [11]. Bediaga *et al.* use the q -deformed statistics to explain the differential cross-section for transverse momenta in electron-positron annihilation [13]. The applications of q -deformed statistics for chaotically quantized scalar fields [14], dark energy [15] are available in the literature. Recently, Das *et al.*[16] found that an ultra-light radion in brane-world Randall-Sundrum model produced in the supernova core can also take away energy released in SN1987A explosion and thus can explain the SN1987A energy loss rate provided q lies within the range $1.18 < q < 1.32$. Here we investigate the supernova SN1987A cooling due to free streaming of fermionic dark matter.

III. DARK MATTER PAIR PRODUCTION INSIDE SUPERNOVA

Electrons are abundant in supernova. The dark matter fermion may be pair produced in the s -channel annihilation of electron and positron: $e^-(p_1)e^+(p_2) \xrightarrow{\gamma} \chi(p_3)\bar{\chi}(p_4)$.

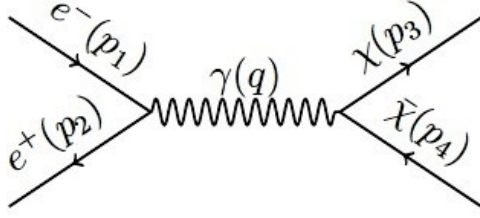


FIG. 1: Feynman diagram for the process $e^-e^+ \xrightarrow{\gamma} \chi\bar{\chi}$

The effective Lagrangian of describing photon(γ) and dark matter fermion (χ) interaction is given by

$$\mathcal{L} = -\frac{i}{2}\bar{\chi}\sigma_{\mu\nu}(\mu_\chi + \gamma_5 d_\chi)\chi F^{\mu\nu} \quad (7)$$

where $F^{\mu\nu} = \partial^\mu A^\nu - \partial^\nu A^\mu$, the e.m.field strength tensor. Here μ_χ and d_χ correspond to the magnetic dipole moment and the electric dipole moment of the dark matter fermion χ . $\sigma^{\mu\nu} = \frac{i}{2}[\gamma^\mu, \gamma^\nu]$ is the spin tensor. The 4-momentum vectors of the initial and final state particles in the centre-of-mass frame are given by

$$\begin{aligned} p_1 &= (E, 0, 0, p_z); \quad p_2 = (E, 0, 0, -p_z); \\ p_3 &= (E', p\sin\theta\cos\phi, p\sin\theta\sin\phi, p\cos\theta); \\ p_4 &= (E', -p\sin\theta\cos\phi, -p\sin\theta\sin\phi, -p\cos\theta). \end{aligned}$$

The spin-averaged amplitude-square for the process $e^-(p_1)e^+(p_2) \xrightarrow{\gamma} \chi(p_3)\bar{\chi}(p_4)$ is given by

$$|\overline{\mathcal{M}}|^2 = 4\pi\alpha[\mu_\chi^2 \{s(1 - \cos^2\theta) + 4m_\chi^2(1 + \cos^2\theta)\} + d_\chi^2 \{(s - 4m_\chi^2)(1 - \cos^2\theta)\}] \quad (8)$$

The differential cross-section for the process is

$$\frac{d\sigma}{d\Omega}(e^-e^+ \xrightarrow{\gamma} \chi\bar{\chi}) = \frac{1}{64\pi^2s} \cdot \sqrt{1 - \frac{4m_\chi^2}{s}} \cdot |\overline{\mathcal{M}}|^2 \quad (9)$$

Finally, the total cross-section is given by

$$\sigma(e^-e^+ \xrightarrow{\gamma} \chi\bar{\chi}) = \frac{\alpha}{6s} \cdot \sqrt{1 - \frac{4m_\chi^2}{s}} \cdot [\mu_\chi^2(s + 8m_\chi^2) + d_\chi^2(s - 4m_\chi^2)] \quad (10)$$

Here m_χ is the dark matter mass, $\alpha = \frac{e^2}{4\pi}$ and $s = (p_1 + p_2)^2 = (p_3 + p_4)^2$ is the Mandelstam variable.

Energy Loss rate

The supernova energy loss rate due to dark matter fermion pair production is given by [5]

$$\begin{aligned}\dot{\epsilon}_{e^-e^+\rightarrow\chi\bar{\chi}} &= \frac{1}{\rho_{SN}} \langle n_{e^-} n_{e^+} \sigma_{e^-e^+\rightarrow\chi\bar{\chi}} V_{rel} E_{com} \rangle \\ &= \frac{1}{\rho_{SN}} \frac{1}{\pi^4} \int_{m_\chi}^{\infty} \int_{m_\chi}^{\infty} dE_1 dE_2 \frac{E_1 E_2 (E_1 + E_2)^3}{2D_1 D_2} \sigma_{e^-e^+\rightarrow\chi\bar{\chi}}\end{aligned}\quad (11)$$

where the c.o.m energy $E_{com}(= E_1 + E_2) = 2E$ (where $E_1 = E_2 = E$) and the relative velocity $V_{rel} = \frac{s}{4E_1 E_2}$. ρ_{SN} is the supernova matter density. The cross-section $\sigma_{e^-e^+\rightarrow\chi\bar{\chi}}$ is given in Eq. 10 and $D_i = \left(1 + \frac{b}{\tau}(E_i - \mu_i)\right)^\tau + 1$ with $i = 1, 2$. Here $b = \frac{\beta_0}{4-3q}$, $\beta_0 = \frac{1}{k_B T}$ (we are working in the unit where $k_B = 1$) and $\tau = \frac{1}{q-1}$. The electron and positron number densities $n_{e^-} = \int \frac{2d^3p_1}{(2\pi)^3} D_1^{-1}$ and $n_{e^+} = \int \frac{2d^3p_2}{(2\pi)^3} D_2^{-1}$. Introducing the dimensionless variables $x_i = E_i/T$ ($i = 1, 2$), we can finally write the energy loss rate Eq. 11 as,

$$\dot{\epsilon}_{e^-e^+\rightarrow\chi\bar{\chi}} = \frac{\alpha T^7}{12\pi^4 \rho_{SN}} \int_{\frac{m_\chi}{T}}^{\infty} dx_1 \int_{\frac{m_\chi}{T}}^{\infty} dx_2 \frac{x_1 x_2 (x_1 + x_2)}{\left[\left(1 + \frac{b}{\tau}(Tx_1 - \mu_{e^-})\right)^\tau + 1\right]} \frac{\mathcal{F}}{\left[\left(1 + \frac{b}{\tau}(Tx_2 - \mu_{e^+})\right)^\tau + 1\right]}\quad (12)$$

where the function \mathcal{F} is given by

$$\mathcal{F} = \sqrt{1 - \frac{4m_\chi^2}{T^2(x_1 + x_2)^2}} \cdot \left[\mu_\chi^2 \left\{ (x_1 + x_2)^2 + \frac{8m_\chi^2}{T^2} \right\} + d_\chi^2 \left\{ (x_1 + x_2)^2 - \frac{4m_\chi^2}{T^2} \right\} \right]\quad (13)$$

Noting the fact that in the $q \rightarrow 1$ limit, the q -deformed distribution formula gets converted to either the Bose-Einstein or Fermi-Dirac statistical distribution formula (which describes the un-deformed scenario) (see the APPENDIX for a proof) i.e.

$$f_i(\beta, E_i) = \frac{1}{(1 + (q-1)bE_i)^{\frac{1}{q-1}} \pm 1} \xrightarrow{q \rightarrow 1} \frac{1}{e^{bE_i} \pm 1} \left(= \frac{1}{e^{\beta_0 E_i} \pm 1} \right)\quad (14)$$

where $e^{bE_i} = e^{\beta_0 E_i}$ with $b = \frac{\beta_0}{4-3q} = \beta_0$ for $q \rightarrow 1$ and β_0 is the inverse equilibrium temperature T_0 of the supernova core, the energy loss rate in $q = 1$ case takes the following form

$$\dot{\epsilon}_{e^-e^+\rightarrow\chi\bar{\chi}} = \frac{\alpha T^7}{12\pi^4 \rho_{SN}} \int_{\frac{m_\chi}{T}}^{\infty} dx_1 \int_{\frac{m_\chi}{T}}^{\infty} dx_2 \frac{x_1(x_1 + x_2)}{\left[\exp\left(x_1 - \frac{\mu_{e^-}}{T}\right) + 1\right]} \frac{x_2}{\left[\exp\left(x_2 - \frac{\mu_{e^+}}{T}\right) + 1\right]} \mathcal{F}\quad (15)$$

where, $\mu_{e^+} = -\mu_{e^-}$

IV. NUMERICAL ANALYSIS

The dark matter produced inside the supernova core via the channel $e^-e^+ \rightarrow \chi\bar{\chi}$ can contribute to the supernova energy loss rate, if the emissivity of this channel $\dot{\epsilon}(e^-e^+ \rightarrow \chi\bar{\chi}) \leq 10^{19} \text{ erg } g^{-1}s^{-1}$ ($= 7.288 \times 10^{-27}\text{GeV}$).

Since the core temperature(T) of the supernova is fluctuating, we follow the χ^2 distribution analysis technique [10] here, where the temperature distribution is characterized by it's mean value $T(= T_{SN}) = 30 \text{ MeV}$ (see Section II B for more details about χ^2 distribution). Because of this temperature fluctuation, the ensemble of nucleons, electrons, dark matter fermions, photons inside the supernova follow a statistics popularly known as the q -deformed statistics (or Tsallis statistics [9], see section II for the related discussion), which is different than the usual Fermi-Dirac and Bose-Einstein statistics. The parameter q characterizing such distribution is called the deformation parameter: for $q \neq 1$, it is the q -deformed distribution, while for $q = 1$, it is the regular Fermi-Dirac or Bose-Einstein distribution (undeformed distribution). We will investigate here the dependence of the deformation parameter q on the scale Λ of the dark matter effective theory for a dark matter fermion of mass lying between $1 - 100 \text{ MeV}$.

A. Bound on the effective scale Λ from the $e^+ + e^- \xrightarrow{\gamma} \chi\bar{\chi}$ process

Depending on whether the effective coupling of dark matter fermion with photon is characterized by a dipole moment operator of magnetic or electric type, we have the below mentioned three cases:

1. Case I: $\mu_\chi(\sim 1/\Lambda_\mu) \neq 0, \quad d_\chi(\sim 1/\Lambda_d) = 0.$
2. Case II: $\mu_\chi(\sim 1/\Lambda_\mu) = 0, \quad d_\chi(\sim 1/\Lambda_d) \neq 0.$
3. Case III: $\mu_\chi(\sim 1/\Lambda_\mu) \neq 0, \quad d_\chi(\sim 1/\Lambda_d) \neq 0.$ Here $\Lambda_\mu = \Lambda_d = \Lambda$

In each case we have two possible scenarios: (i) Scenario I: The deformation parameter $q > 1$ which is known as the q -deformed scenario and (ii) Scenario II: The deformation parameter $q = 1$ which is the undeformed scenario and particles obey the usual Fermi-Dirac or Bose-Einstein statistics.

1. Scenario I: q -deformed statistics ($q > 1$)

Using the Raffelt's criteria $\dot{\epsilon}(e^-e^+ \rightarrow \chi\bar{\chi}) \leq 10^{19} \text{ erg } g^{-1}s^{-1}$ ($= 7.288 \times 10^{-27} \text{ GeV}$) and equation (12), we derive a lower bound on the scale Λ (which we denote as Λ_μ and Λ_d in Case I and Case II, respectively) of the dark matter effective theory. In Fig. 2, we have plotted Λ_μ, Λ_d (Case I, Case II) and Λ (Case III) as a function of the dark matter fermion mass m_χ corresponding to $q = 1.05$ (left figure) and $q = 1.1$ (right figure), respectively. The region

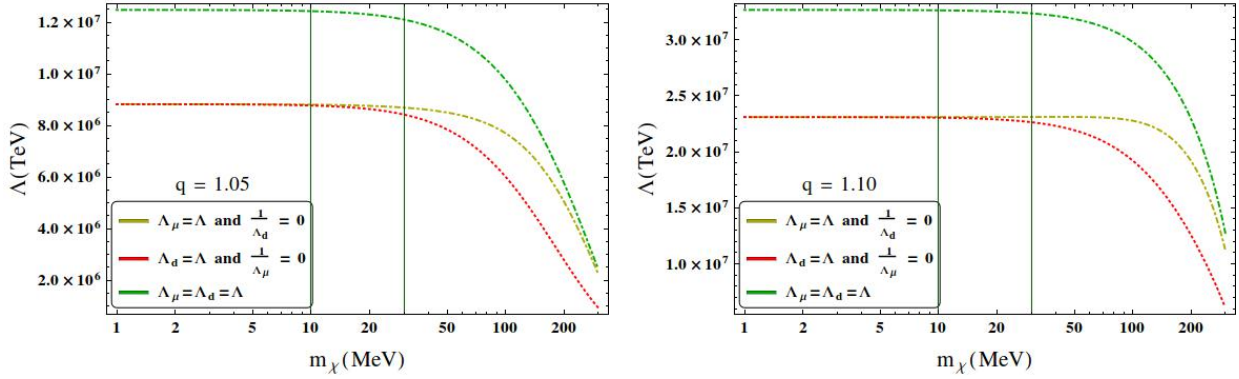


FIG. 2: $\Lambda_{\mu,d}$ (in TeV) (lower two curves) and Λ (in TeV) (topmost curve) are plotted against m_χ (in MeV) for $q = 1.05$ (left figure) and $q = 1.1$ (right figure), respectively.

lying on the left of the vertical line corresponding to $m_\chi = 30$ MeV and above the horizontal curves of each figure is allowed. For $10 \text{ MeV} \leq m_\chi \leq 30 \text{ MeV}$ [6], the effective scale Λ corresponding to that window (and above the curves) is allowed. Note that $\Lambda_{\mu,d}$ remains constant (in both figures) till $m_\chi = 10$ MeV and starts decreasing after that. On the left figure ($q = 1.05$), till $m_\chi = 10$ MeV we find $\Lambda_\mu = \Lambda_d = 8.8 \times 10^6$ TeV (Case I and Case II) and $\Lambda = 1.24 \times 10^7$ TeV (Case III). It becomes $\Lambda_\mu = 8.7 \times 10^6$ TeV and $\Lambda_d = 8.4 \times 10^6$ TeV (in Case I and Case II) and $\Lambda = 1.2 \times 10^7$ TeV (in Case III) at $m_\chi = 30$ MeV. As we go from left to right figure, $\Lambda_{\mu,d}$ gets increased at a given m_χ . For $m_\chi = 30$ MeV, the topmost curve gives $\Lambda = 3.23 \times 10^7$ TeV, whereas the lower two curves give $\Lambda_\mu = 2.3 \times 10^7$ TeV and $\Lambda_d = 2.26 \times 10^7$ TeV, respectively.

In Fig. 3 we have shown Λ as a function of the deformation parameter q corresponding to $m_\chi = 5, 10, 20$ and 30 MeV for the above three cases (using Raffelt's criteria and analyzing the equation (12)). On the right figure, the same plots are shown corresponding to $1.0 \leq q \leq 1.04$. The following observations are in order:

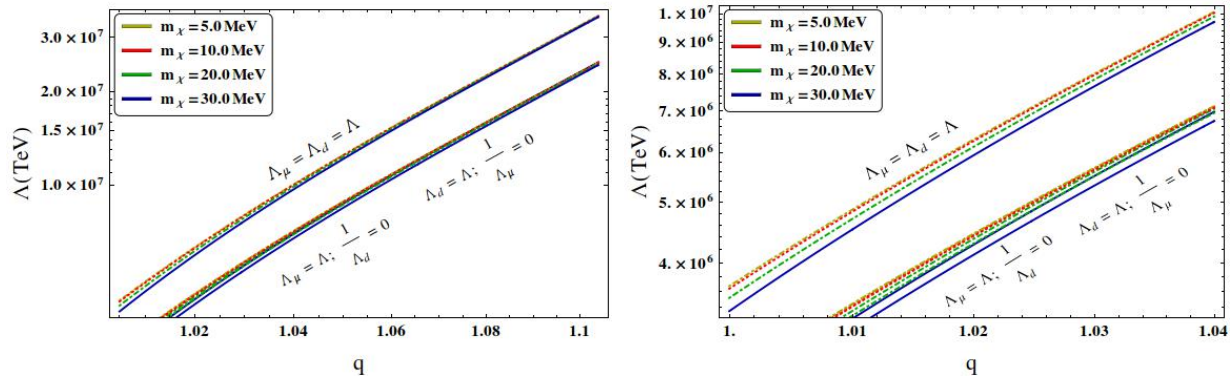


FIG. 3: In the left figure, $\Lambda_{\mu,d}$ (in TeV) (lower curves) and Λ (in TeV) (upper curves) are plotted as a function of q for $m_\chi = 5, 10, 20$ and 30 MeV. On the right, we have plotted the same but for $1.04 < q < 1$.

1. For a given m_χ , the lower bound on Λ increases as q increases. For example, for $m_\chi = 30$ MeV, Λ changes from 4.8×10^6 TeV to 3.4×10^7 TeV as q changes from 1.01 to 1.1 (left figure).
2. For a given q , Λ decreases with the increase in m_χ . For example, for $q = 1.03$, we see that as m_χ increases from 10 MeV to 30 MeV, Λ decreases from 8×10^6 TeV to 7.7×10^6 TeV.

2. Scenario II: Undeformed statistics($q = 1$)

The q -deformed distribution becomes the usual(undeformed) Bose-Einstein or Fermi-Dirac type distribution for $q = 1$ (in Appendix A, we have given a derivation of this). We are now to investigate how the bound on Λ gets changed as one switches from a deformed distribution to an un-deformed distribution. In Fig. 4, we have plotted $\Lambda_{\mu,d}$ and Λ against m_χ for $q = 1$ using the Raffelt's criteria and equation (15). The region on the left of the vertical line at $m_\chi = 30$ MeV and above the horizontal curves is allowed. Up to $m_\chi = 10$ MeV, we find Λ_μ (Case I) and Λ_d (Case II) are found to be constant at $\sim 2.6 \times 10^6$ TeV and after which they start decreasing. The topmost curve corresponds to Λ (Case III) for different values of m_χ . For example, corresponding to $m_\chi = 1 - 10$ MeV, we find $\Lambda \sim 3.6 \times 10^6$ TeV, while at $m_\chi = 30$ MeV, we find $\Lambda = 3.3 \times 10^6$ TeV. We have summarized our result in Table 1. From Table 1, we see that as m_χ increases, the bound on $\Lambda_{\mu,d}$ and Λ decreases.

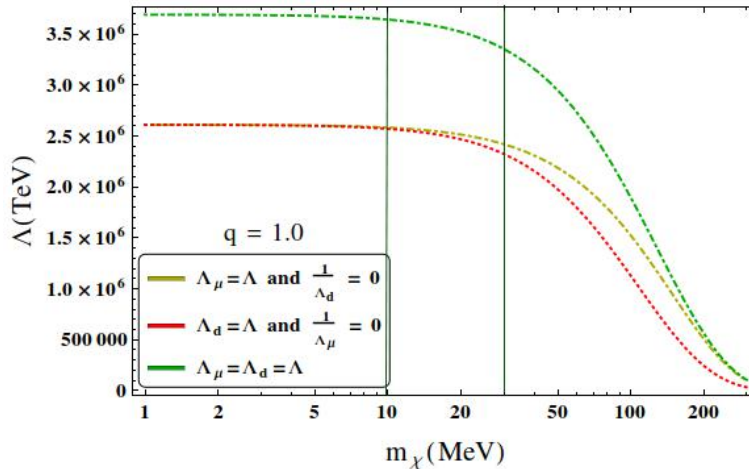


FIG. 4: $\Lambda_{\mu,d}$ (in TeV) and Λ (in TeV) are plotted against m_χ (in MeV) for $q = 1$.

Table 1

m_χ (MeV)	Case I : Λ_μ (TeV)	Case II : Λ_d (TeV)	Case III : Λ (TeV)
10	2.6×10^6	2.6×10^6	3.6×10^6
30	2.4×10^6	2.3×10^6	3.3×10^6

Table 1: The lower bound on the effective scale Λ_μ , Λ_d and Λ (TeV) are shown for different dark matter mass m_χ (MeV) in the undeformed scenario.

The lower bound obtained on Λ_μ is comparable with that obtained by Kadota *et al.*[17].

V. DARK PARTICLE FREE STREAMING/TRAPPING

The constraint on Λ obtained in earlier section holds to be true if the produced dark matter fermion free streams out of the supernova. To find the free streaming let us calculate their mean free path [18]

$$\lambda_\chi = \frac{1}{n_e \cdot \sigma_{e\chi \rightarrow e\chi}} \quad (16)$$

where $n_e (= 8.7 \times 10^{43} m^{-3})$ is the number density of the colliding electrons in the supernova and $\sigma_{e\chi \rightarrow e\chi}$ is the cross section for the scattering of dark matter fermion on electron which is related via the crossing symmetry to the annihilation cross-section $\sigma_{ee \rightarrow \chi\chi}$. Now, most of the dark matter particles produced in the outermost 10% of the star ($0.9R_c < r < R_c$) from electron-positron annihilation [19]. Then any of the dark matter particles produced

in electron-positron annihilation while propagating through the proto-neutron star, can undergo scattering due the presence of neutrons and electrons inside the star. In the case of supernova cooling, neutron-dark matter particle scattering will be negligible for free streaming due to neutron mass [18]. We use the optical depth criteria [18]

$$\int_{r_0}^{R_c} \frac{dr}{\lambda_\chi} \leq \frac{2}{3} \quad (17)$$

to investigate whether the dark matter fermion produced at a depth r_0 free streams out of the supernova and takes away the released energy or getting trapped inside the supernova. Here we set $r_0 = 0.9R_c$ in our analysis, where $R_c(\simeq 10 \text{ km})$ is the radius of the supernova core (proto-neutron star) [18]. From the optical depth criteria, we find that minimum length of the mean free path for free streaming λ_{fs} is $\lambda_{fs}^{min} = 1.5 \text{ km}$ and it increases with Λ . In

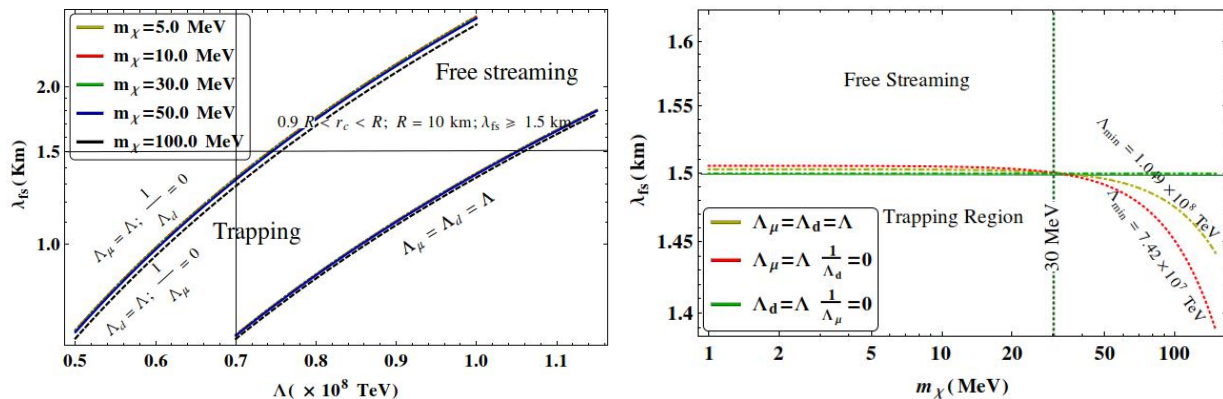


FIG. 5: On the left side, the free streaming length λ_{fs} (km) is plotted as a function of Λ (GeV) for different m_χ . We have taken $R_c(= R) = 10 \text{ km}$. On the right side, the free streaming length λ_{fs} (km) is plotted as a function of m_χ (MeV). The trapping and free streaming regions are shown separately.

Fig. 5(on the left side), we have shown the free streaming length λ_{fs} (in km) as a function of Λ for different m_χ . Results for three different cases: Case I: $\Lambda_\mu = \Lambda, \frac{1}{\Lambda_d} = 0$ and Case II: $\Lambda_d = \Lambda, \frac{1}{\Lambda_\mu} = 0$ and Case III: $\Lambda_\mu = \Lambda_d = \Lambda$ are shown. The horizontal line correspond to $\lambda_{fs}^{min} = 1.5 \text{ km}$ and it's intersection with the curves gives the lower bound on $\Lambda_\mu(\Lambda_d) = 7.42 \times 10^7 \text{ TeV}$, in Case I (Case II) and $\Lambda = 1.05 \times 10^8 \text{ TeV}$ in Case III, respectively. On the right side (of Figure 5), we have plotted the free streaming length λ_{fs} against m_χ . The horizontal lines corresponding to $\lambda_{fs}^{min} = 1.5 \text{ km}$ remain constant until

$m_\chi = 30$ MeV, after which they start decreasing except the Case-II in which it remains to be constant beyond $m_\chi = 30$ MeV. The region below the line $\lambda_{fs} = 1.5$ km corresponds to the trapping region, whereas the region above this horizontal line corresponds to the free streaming region. In Case II, where the dark matter-electron coupling is due to electric dipole moment of the dark matter fermion, the free streaming of dark matter particles is allowed for the entire mass range and thus are not trapped inside the supernova. In Fig. 6, we have plotted the lower bound on Λ against the dark matter mass m_χ (considering $T_{SN} = 30$ MeV, $\rho_{SN} = 3 \times 10^{14}$ gm/cc, $n_e = 8.7 \times 10^{43}$ m $^{-3}$).

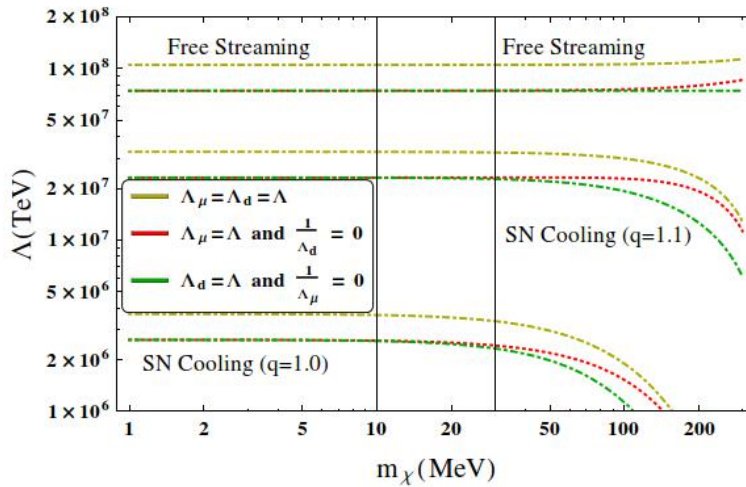


FIG. 6: Λ (in TeV) is plotted against m_χ (MeV). The lower set of curves follow from the SN1987A cooling in undeformed scenario($q=1.0$), while the upper set of curves follows from the free streaming of dark matter fermions from the supernova core. The middle set of curves follows from the SN1987A cooling in q -deformed scenario($q=1.1$).

The upper(most) set of curves corresponds to that obtained using optical depth criteria (based on free streaming of dark matter fermion from the supernova core), whereas the lower(most) set of curves are obtained after applying the Raffelt's criteria on the SN1987A energy loss rate in undeformed case and the set of curves in the middle are obtained from the SN1987A cooling in q -deformed scenario($q=1.1$). The region above both the curves (free streaming and SN cooling) is allowed for two different scenarios, $q=1.0$ and $q=1.1$. correspond to $m_\chi = 10$ MeV and 30 MeV. For a dark matter of mass $m_\chi = 30$ MeV, the SN1987A energy loss rate gives a lower bound $\Lambda(= \Lambda_\mu) = 2.4 \times 10^6$ TeV (lower curve) in undeformed scenario($q=1.0$) and $\Lambda(= \Lambda_\mu) = 2.3 \times 10^7$ TeV (lower curve) in q -deformed

scenario($q=1.1$), whereas optical depth criterion (i.e. free streaming) fixes the lower bound on $\Lambda(=\Lambda_\mu)$ at 7.42×10^7 TeV (lower curve).

VI. DEPENDENCY OF THE EFFECTIVE SCALE Λ ON THE SUPERNOVA PROPERTIES

So far in our discussions we have not considered the variation of supernova properties like temperature(T_{SN}), matter density(ρ_{SN}), number density of electron(n_e) which are relevant in the $e\chi \rightarrow e\chi$ scattering process and on the variation of the lower bound on the effective scale Λ . The analysis was based on the following assumptions

$$T_{SN} = 30 \text{ MeV}, \quad \rho_{SN} = 3 \times 10^{14} \text{ gm/cc}, \quad n_e = 8.7 \times 10^{43} \text{ m}^{-3}$$

where, we considered T_{SN} is the average temperature of the supernova, ρ_{SN} is the average matter density of the supernova and n_e is the number density of the colliding electrons in the supernova (which are taking part in the $e\chi \rightarrow e\chi$ scattering process).

In the analysis below, we propose the following

- (i) We can look for the fermionic DM emission pattern which is consistent with the Kamiokande [7] and IMB [8] data for neutrino emission due to supernova SN1987A explosion (which is more relevant as per our current understanding of supernova explosion mechanism).
- (ii) In another possibility, we can think about the annihilation process $e^-e^+ \rightarrow \chi\bar{\chi}$ which is happening only at the outer 10% of the proto-neutron star at some higher temperature (say 50 MeV) and some lower density (say $\rho_{SN} = 10^{14}$ gm/cc) [19–23]. The justification of this second possible assumption is due to infall of matter particles in the accretion phase of the supernova, temperature is increasing at the outermost (10%) region of the supernova core. Also due to the electron capture process by the protons, the central region of the proto-neutron star will be neutron-rich region and will not have much free electron-positron pair which can take part in the annihilation process.

A. Case I

We can consider the supernova cooling phenomena due to the free streaming of dark matter fermions in both the phases, accretion phase and Kelvin-Helmholtz cooling phase. Due to infall of the matter objects in the accretion phase the temperature at the outermost region will increase than the average. The number density(n_e) of the colliding electron (which takes part in $e\chi \rightarrow e\chi$ scattering process) although appears to increase due to infall but actually not so. The infall boosts the production process of dark fermions(due to electron-positron annihilation: $e^-e^+ \rightarrow \chi\bar{\chi}$) and the electron capture process by protons to create a neutron-rich core- together (annihilation and capture processes) result the number density(n_e) to fall to a lower value.

In Fig. 7, we have plotted the electron number density n_e (in m^{-3}) against the mean free path λ_{fs} (in km) for $q = 1.0$ (undeformed scenario) and $q = 1.1$ (deformed scenario), respectively.

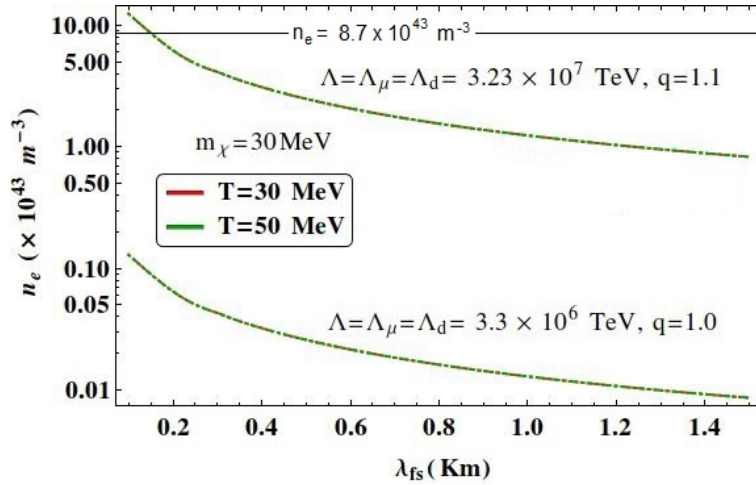


FIG. 7: The electron number density n_e (in m^{-3}) is plotted against the electron's mean free path λ_{fs} (in km). We have taken the dark matter fermion of mass $m_\chi = 30$ MeV and the value of the deformation parameter $q = 1.0$ (lower curve) and $q = 1.1$ (upper curve), respectively.

We have considered the average supernova temperature $T = 30$ MeV and the number density $n_e = 8.7 \times 10^{43} m^{-3}$ [18]. Considering the fact that the dark matter fermions, produced at a depth $r_0 = 0.9R_c$, free stream out of the supernova and take away the released energy, we find (from the optical depth criterion [18]) that the minimum length of the mean free path for free streaming (λ_{fs}) is $\lambda_{fs}^{min} = 1.5$ km.

From figure[7], we see that if the value of the mean free path ~ 1.5 km, we need to choose $n_e \sim 10^{41} \text{ m}^{-3}$ in the undeformed scenario($q=1.0$) and $n_e \sim 10^{43} \text{ m}^{-3}$ in the q -deformed scenario($q=1.1$), respectively. Suppose at the outermost region the number density drops to $\sim 10^{43} \text{ m}^{-3}$ (from the average value $8.7 \times 10^{43} \text{ m}^{-3}$) and temperature rises to $T = 50 \text{ MeV}$ (above the average value $T = 30 \text{ MeV}$) which is consistent with existing supernova simulation (matter density also decreases from its average value $3 \times 10^{14} \text{ gm/cc}$ to 10^{14} gm/cc) [20] (we compared with the s23WH07 model as in that model mass of the progenitor was considered to be $23M_\odot$ and progenitor of SN1987A had mass $\sim 20M_\odot$). In Fig. 8, we have plotted the lower bound on Λ against the dark matter mass m_χ (obtained from the supernova energy loss rate and from the free streaming of the produced dark

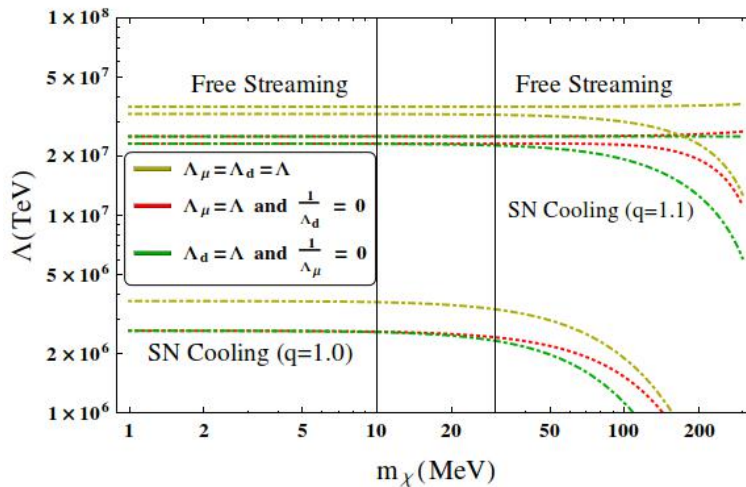


FIG. 8: The lower bound on Λ (in TeV) (obtained from energy loss rate and the free streaming criteria) is plotted against m_χ (in MeV). The lower set of curves follows from the SN1987A cooling for $q=1.0$ and $T_{SN} = 30 \text{ MeV}$, while the curves in the above follow from the free streaming of dark matter fermions from the outermost region of the supernova core. The SNe cooling curves in q -deformed scenario($q=1.1$) (the curves in the middle) are almost overlapping with the curves followed from free streaming.

fermions from the outermost region of the supernova core). The free streaming process is insensitive to the temperature T_{SN} , we set $\rho_{SN} = 3 \times 10^{14} \text{ gm/cc}$ and $n_e = 1 \times 10^{43} \text{ m}^{-3}$ in the free streaming case.

The upper set of curves are obtained from the optical depth criteria (based on free streaming of dark matter fermion from the outermost part of the supernova core), whereas

the lower set of curves are obtained by applying the Raffelt's criteria on the SN1987A energy loss rate. The free streaming curves have shifted downwards from the one obtained in figure[6] and the SN cooling curves in q-deformed scenario($q=1.1$) is almost merging with the set of curves for free streaming. The two vertical lines correspond to $m_\chi = 10$ MeV and 30 MeV, respectively. For a dark matter of mass $m_\chi = 30$ MeV, the SN1987A energy loss rate gives a lower bound $\Lambda(= \Lambda_\mu = \Lambda_d) = 3.3 \times 10^6$ TeV (upper curve) in the undeformed scenario($q=1.0$) and $\Lambda(= \Lambda_\mu = \Lambda_d) = 3.2 \times 10^7$ TeV (upper curve) in the deformed scenario($q=1.1$), whereas the optical depth criterion (i.e. free streaming) fixes the lower bound on $\Lambda(= \Lambda_\mu = \Lambda_d)$ at 3.6×10^7 TeV (upper curve). This suggests almost all of the produced dark matter fermions can freely stream out of supernova to contribute to the supernova cooling with the fact that they are obeying q-deformed statistics: $q=1.1$ and with $n_e = 1 \times 10^{43} \text{ m}^{-3}$), which was not the case for $T = 30$ MeV in undeformed scenario.

For the crust temperature $T = 50$ MeV and the number density of colliding electron $n_e = 10^{43} \text{ m}^{-3}$ we have plotted the mean free path(λ_{fs}) as a function of the effective scale(Λ) and temperature(T) in figure[9] for different values of dark matter fermion mass m_χ .

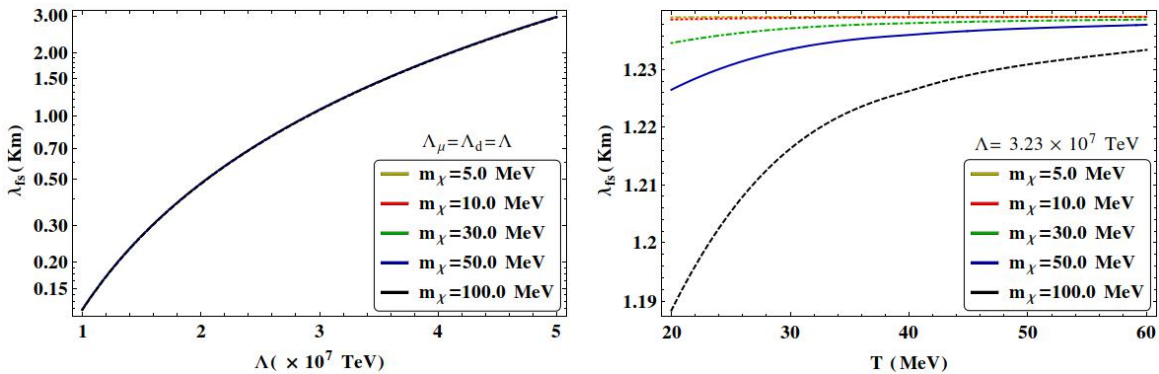


FIG. 9: In the left figure λ_{fs} (in km) is plotted against Λ (in TeV) for $T = 50$ MeV whereas in the right figure λ (in km) is plotted against T (in MeV) for $\Lambda_\mu = \Lambda_d = \Lambda = 3.23 \times 10^7$ TeV (bound obtained from the SN cooling case in q-deformed scenario with $q=1.1$).

In figure[9](left) we see that the mean free path λ_{fs} increases with the effective scale Λ for different dark matter fermion mass. On the right, we see that it first increases with temperature but eventually becomes constant with temperature T and they are different for different m_χ (GeV).

We next study the variation of the effective scale Λ with temperature for different mass of

dark matter fermions for a given λ_{fs} and different values of mean free path for a given m_χ and are shown in figure[10]. From figure[10] it is clear that the effective scale Λ varies feebly with

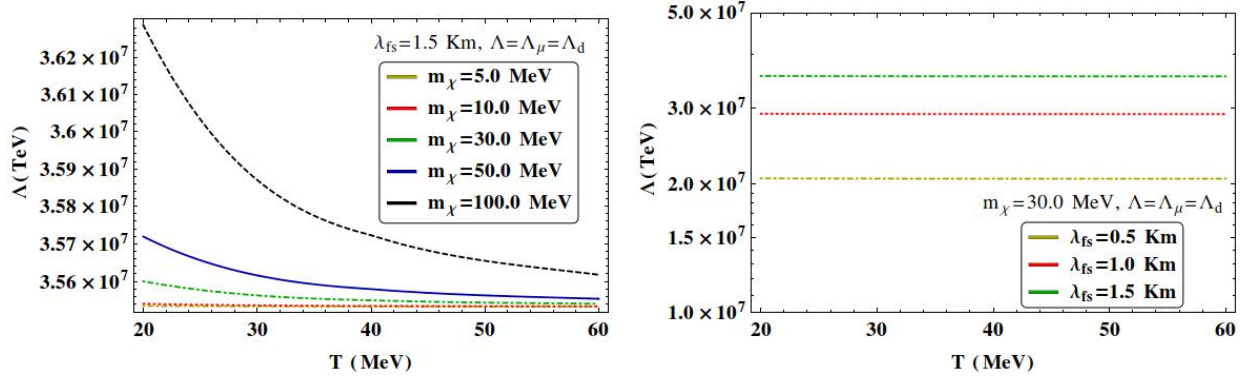


FIG. 10: $\Lambda = \Lambda_\mu = \Lambda_d$ (in TeV) is plotted against T (in MeV) where we have chosen $n_e = 10^{43} \text{ m}^{-3}$. The left figure corresponds to the variation of Λ with respect to T for fixed mean free path $\lambda = 1.5$ km and for different m_χ whereas the right figure shows the variation of Λ with respect to T for different mean free path λ (in km) and for fixed $m_\chi = 30$ MeV.

temperature, it remains almost constant. Variation of the effective scale Λ with the number density of colliding electrons n_e (which are taking part in the $e\chi \rightarrow e\chi$ scattering process) has been shown in figure[11]. We find that Λ increases considerably with the increment of the

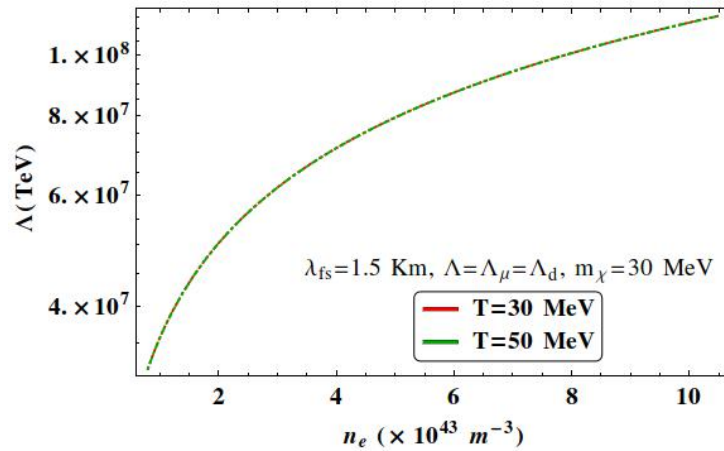


FIG. 11: The effective scale $\Lambda = \Lambda_\mu = \Lambda_d$ (in TeV) obtained for free streaming cases (using eqn.[16]) is plotted against n_e (in m^{-3}) for $\lambda_{fs} = 1.5$ km, $m_\chi = 30$ MeV. We find $\Lambda \sim 4 \times 10^7$ TeV for $n_e = 10^{43} \text{ m}^{-3}$ and $\Lambda \sim 1 \times 10^8$ TeV for $n_e = 8.7 \times 10^{43} \text{ m}^{-3}$.

number density of colliding electrons n_e (which are relevant in the discussion of the $e\chi \rightarrow e\chi$

scattering process). For $n_e = 10^{43} \text{ m}^{-3}$, we find $\Lambda \sim 4 \times 10^7 \text{ TeV}$ and for $n_e = 8.7 \times 10^{43} \text{ m}^{-3}$, $\Lambda \sim 1 \times 10^8 \text{ TeV}$.

B. Case II

In section V, we considered the supernova core temperature $T_{SN} = 30 \text{ MeV}$ and the core density as $\rho_{SN} = 3 \times 10^{14} \text{ gm/cc}$. From the equations (12, 13) it is clear that, the lower bound on the effective scale Λ depends on the properties (temperature and density) of the supernova. As free streaming is happening from the outermost 10% of the supernova core, so it is justified to consider only crust (i.e., crust temperature and density) in the discussion of the supernova cooling phenomena as well. For core-collapse supernova, the crust temperature will be higher than the core whereas the density will fall from core to crust [20, 24, 25]. In this section, we calculate the lower bound on Λ in un-deformed ($q = 1$) scenario using Raffelt's criteria and equation (15) considering temperature $T = 50 \text{ MeV}$ and density $\rho = 10^{14} \text{ gm/cc}$ at the outermost sector (i.e. at $r = 0.9 R_c$, the crust) of the supernova core.

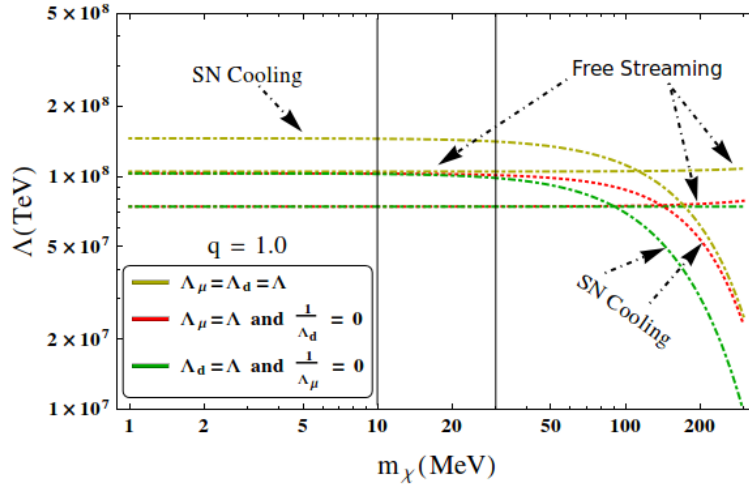


FIG. 12: The lower bound $\Lambda = \Lambda_\mu = \Lambda_d$ (TeV) (in TeV) is plotted against the dark matter fermion mass m_χ (MeV) for two cases: (i) free streaming of dark matter fermions from the crust and (ii) from the Raffelt's criteria of SN1987A energy loss rate.

In Fig. 12, we plot the lower bound on $\Lambda (= \Lambda_\mu = \Lambda_d)$ (TeV) as a function of m_χ . The almost parallel set of curves (also parallel to x-axis) obtained using optical depth

criteria (based on the free streaming of dark matter fermion from the outermost sector of the supernova core), whereas the other set of curves are obtained after applying the Raffelt's criteria on the SN1987A energy loss rate (equation[15]). The region above each curve is allowed. The two vertical lines correspond to $m_\chi = 10$ MeV and 30 MeV. For a dark matter of mass $m_\chi = 30$ MeV, the SN1987A energy loss rate gives a lower bound $\Lambda(= \Lambda_\mu = \Lambda_d) = 1.42 \times 10^8$ TeV (upper curve), whereas optical depth criterion (i.e. free streaming) fixes the lower bound on $\Lambda(= \Lambda_\mu = \Lambda_d)$ at 1.05×10^8 TeV (upper curve). Note that the dark matter fermions produced in the outermost sector(i.e. at $0.9R_c$) can freely stream out to contribute in the supernova cooling phenomena which is not the case if they are produced at some inner region (i.e. at distance $r < 0.9R_c$) of the supernova core. Even they are be copiously produced, they are not allowed to free stream (restricted by optical depth criterion) and hence can't contribute to the SN cooling as is seen from Figure[6]. Some of them will transfer part of its energy back to the medium via scattering and as a result, the cooling process occurs slowly.

Below in Table 2 and Table 3, we summarize our result and make a comparative study between two cases as discussed in section V and section VI:

Table 2

SN Properties	m_χ (MeV)	$\Lambda = \Lambda_\mu = \Lambda_d$ (TeV)	
		Free Streaming	SN Cooling
$T_{SN} = 30$ MeV, $\rho = 3 \times 10^{14}$ gm/cc	10	1.05×10^8	3.66×10^6
	30	1.05×10^8	3.34×10^6
$T_{SN} = 50$ MeV, $\rho = 10^{14}$ gm/cc	10	1.05×10^8	1.45×10^8
	30	1.05×10^8	1.42×10^8

Table 2: The lower bound on the effective scale $\Lambda = \Lambda_\mu = \Lambda_d$ (TeV) (obtained from Raffelt's criteria and optical depth criterion) are shown for different dark matter mass m_χ (MeV) in the undeformed scenario for different values of SN temperature $T(= T_{SN})$ and matter density ρ_{SN} .

From Table 2, we see that as m_χ increases from 10 MeV to 30 MeV, the bound on Λ decreases (follows from SN energy loss rate) whereas for free streaming case (optical depth criterion) Λ remains constant. We also see from Table 2 that the bound on Λ change as a function of the supernova properties (i.e. it's temperature and density). In Table 3, we have

shown the lower bound $\Lambda = \Lambda_\mu = \Lambda_d$ (TeV) (obtained from Raffelt's criteria and optical depth criterion) for different dark matter mass m_χ (MeV) in the undeformed scenario and q -deformed scenario for different values of supernova crust temperature T and different values of the electron density n_e .

Table 3

SN Properties	m_χ (MeV)	$\Lambda = \Lambda_\mu = \Lambda_d$ (TeV)		
		Free Streaming	SN Cooling($q=1.0$)	SN Cooling($q=1.1$)
$T = 30$ MeV, $n_e = 8.7 \times 10^{43} \text{ m}^{-3}$	10	1.05×10^8	3.66×10^6	3.23×10^7
	30	1.05×10^8	3.34×10^6	3.23×10^7
$T = 50$ MeV, $n_e = 1 \times 10^{43} \text{ m}^{-3}$	10	3.6×10^7	3.66×10^6	3.23×10^7
	30	3.6×10^7	3.34×10^6	3.23×10^7

Table 3: The lower bound on the effective scale $\Lambda = \Lambda_\mu = \Lambda_d$ (TeV) (obtained from Raffelt's criteria and optical depth criterion) are shown for different dark matter mass m_χ (MeV) in the undeformed scenario and q -deformed scenario for different values of SN crust temperature T . We have considered the variation of the temperature and the number density of colliding electrons n_e only at the crust level.

If we consider different phases of a typical core-collapse supernova like the accretion and Kelvin-Helmholtz cooling phase, then the bounds will change. We can compare the bounds with the knowledge of temperature and density of supernova in those phases.

VII. CONCLUSION

The dark matter fermions, pair produced in electron-positron collision $e^+e^- \rightarrow \chi\bar{\chi}$ inside the supernova core, can take away the energy released in the supernova SN1987A explosion. Working within the formalism of q -deformed statistics (as the core supernovae temperature is fluctuating with the average value $T_{SN} = 30$ MeV) and using the Raffelt's criterion on the emissivity for any new channel $\dot{\epsilon}(e^+e^- \rightarrow \chi\bar{\chi}) \leq 10^{19} \text{ erg } g^{-1}s^{-1}$, we find that as the deformation parameter q changes from 1.0 (undeformed scenario) to 1.1(deformed scenario), the lower bound on the scale Λ of the dark matter effective theory varies from 3.3×10^6 TeV to 3.2×10^7 TeV for a dark matter fermion of mass $m_\chi = 30$ MeV. Using the optical depth criteria on the free streaming of the dark matter fermion, we find the lower bound

on $\Lambda \sim 10^8$ TeV for $m_\chi = 30$ MeV. In a scenerio, where the dark matter fermions are pair produced in electron-positron annihilation in the outermost sector of the supernova core (with radius $0.9R_c \leq r \leq R_c$ where $R_c (= 10 \text{ km})$ being the supernova core radius or the radius of proto-neutron star), we find that the bound on Λ ($\sim 3 \times 10^7$ TeV) obtained from SN cooling criteria (Raffelt's criteria) is comparable with the bound obtained from free streaming (optical depth criterion) for light fermion dark matter of mass $m_\chi = 10 - 30$ MeV. In a nutshell, all the dark matter fermions produced in the outermost sector (i.e. at the crust) can freely stream out to contribute to the supernova cooling phenomena which is not the case if they are producing in some inner region than the crust.

VIII. ACKNOWLEDGMENTS

The authors would like to thank Dr. Partha Konar, PRL, Ahmedabad and Prof. Debasish Majumdar, SINP, Kolkata and Prof. Tirthankar Roychaudhury for discussions. This work is partially funded by the Board of Research in Nuclear Science, Department of Atomic Energy, Government of India, Grant No. 2011/37P/08/BRNS.

IX. FEYNMAN RULES

Process: $e^- e^+ \xrightarrow{\gamma} \chi \bar{\chi}$:

$e^- e^+ \rightarrow \gamma$ vertex: $ie\gamma^\mu$

$\gamma \rightarrow \chi \bar{\chi}$ vertex: $i(\mu_\chi \sigma^{\mu\nu} q_\nu + d_\chi \sigma^{\mu\nu} q_\nu \gamma^5)$

X. APPENDIX:

From q-deformed statistics to undeformed scenario

In general, the distribution function for the q-deformed statistics is [9]

$$D_i = \left(1 + \frac{b}{\tau}(E_i - \mu_i)\right)^\tau + 1 \quad (18)$$

with $b = \frac{\beta_0}{4-3q}$, $\beta_0 = \frac{1}{k_B T}$ (we work in the unit $k_B = 1$) and $\tau = \frac{1}{q-1}$

In terms of the dimensionless quantity $x_i = \frac{E_i}{T}$

$$D_i = (1 + b(q-1)(Tx_i - \mu_i))^{\frac{1}{q-1}} + 1 \quad (19)$$

Now replacing $q - 1$ by m , ($m \rightarrow 0$ as $q \rightarrow 1$)

$$(1 + b(q - 1)(Tx_i - \mu_i))^{\frac{1}{q-1}} = (1 + bm(Tx_i - \mu_i))^{\frac{1}{m}} = y(\text{say}) \quad (20)$$

Now

$$\begin{aligned} \lim_{m \rightarrow 0} y &= \lim_{m \rightarrow 0} (1 + bm(Tx_i - \mu_i))^{\frac{1}{m}} \\ \implies \lim_{m \rightarrow 0} \ln y &= \lim_{m \rightarrow 0} \frac{1}{m} \ln (1 + bm(Tx_i - \mu_i)) \\ &= \lim_{m \rightarrow 0} \frac{1}{1 + bm(Tx_i - \mu_i)} b(Tx_i - \mu_i) \\ &= b(Tx_i - \mu_i) \end{aligned}$$

Also for $q \rightarrow 1$, we find $b(= \frac{\beta_0}{4-3q}) = \beta_0 = \frac{1}{k_B T} = \frac{1}{T}$. So we find

$$\begin{aligned} \lim_{q \rightarrow 1} \ln y &= \beta_0(Tx_i - \mu_i) \\ \implies \lim_{q \rightarrow 1} y &= \exp \left[\frac{1}{T}(Tx_i - \mu_i) \right] \\ &= \exp \left[x_i - \frac{\mu_i}{T} \right] \end{aligned}$$

Clearly, in the undeformed scenario (i.e. $q = 1$)

$$\begin{aligned} \lim_{q \rightarrow 1} D_i &= \lim_{q \rightarrow 1} y + 1 \\ &= \exp \left[x_i - \frac{\mu_i}{T} \right] + 1 \quad [Proved] \end{aligned} \quad (21)$$

-
- [1] F. Zwicky, *Helv. Phys. Acta* **6**, 110 (1933).
 - [2] J. L. Feng *Ann. Rev. Astron. Astrophys.* **48**, 495, 2010 [arXiv:1003.0904].
 - [3] G. Jungman, M. Kamionkowski, K. Griest, *Phys. Rept.* **267**, 195-373 (1996). [hep-ph/9506380]
 - [4] G. Bertone, D. Hooper, J. Silk, *Phys. Rept.* **405**, 279-390 (2005). [hep-ph/0404175].
 - [5] G. G. Raffelt, *Stars as Laboratories for Fundamental Physics*, (Chicago University Press) (1996).
 - [6] P. Fayet, D. Hooper and G. Sigl. *Phys. Rev. Lett.* **96**, 211302 (2006).
 - [7] K. Hirata et.al., *Phys. Rev. Lett.* **58**, 1490 (1987).

- [8] R. M. Bionta et.al., Phys. Rev. Lett. **58**, 1494 (1987).
- [9] C. Tsallis, J. Stat. Phys. **52**, 479 (1988).
- [10] C. Beck, E. G. D. Cohen, Physica A **322**, 267 (2003).
- [11] C. Beck, Eur. Phys. A **40**, 267-273 (2009).
- [12] C. Beck, Physica A **331**, 173 (2004).
- [13] I. Bediaga, E.M.F. Curado, J.M. de Miranda, Physica A 286 (2000) 156.
- [14] C. Beck, Nonlinearity **8**, 423 (1995).
- [15] C. Beck, Phys. Rev. D **69**, 123515 (2004).
- [16] Prasanta Kr. Das *et al.* Int.J.Mod.Phys. A **28**, 1350152 (2013).
- [17] Kenji Kadota and Joseph Silk, Phys. Rev. D **89**, 103528 (2014).
- [18] H. K. Dreiner, J. F. Fortin, C. Hanhart and L. Ubaldi, Phys. Rev. D **89**, 105015 (2014).
- [19] H. K. Dreiner, C. Hanhart, U. Langenfeld and D. R. Phillips, Phys. Rev. D **68**, 055004 (2003).
- [20] Prasanta Char, Sarmistha Banik and Debades Bandyopadhyay, Astrophys.J., **809:116** (2015).
- [21] J. R. Ellis, K. A. Olive, S. Sarkar and D. W. Sciama, Phys. Lett. B **215** (1988) 404.
- [22] K. Lau, Phys. Rev. D **47** (1993) 1087.
- [23] Prasanta Kumar Das, V. H. Satheeshkumar and P. K. Suresh, Phys. Rev. D **78**, 063011 (2008).
- [24] Kohsuke Sumiyoshi and Gerd Ropke, Phys. Rev. C **77**, 055804 (2008).
- [25] K. Hagel, J. B. Natowitz, and G. Ropke, Eur. Phys. J. A (2014) 50:39.
- [26] Atanu Guha, Selvaganapathy J and Prasanta Kumar Das, *Work in progress*.